A numerical study of the Ecovat with IFISS

Sagy Ephrati, Henk Jonker*

University of Twente

June 30, 2017

1. Introduction

Climate change is a much-discussed topic nowadays. A shift from traditional fossil fuels to renewable 'green' energy is happening on a large scale. The production of this renewable energy such as solar energy and wind energy cannot be controlled by human activities, which results in either too much or too little energy produced at each moment in time.

The Ecovat offers a solution to this problem by using thermal energy storage. Water is stored in layers of different temperatures in a closed, subterranean vessel. Energy can be stored and extracted by charging and discharging at different temperatures on multiple possible places in the wall of the vessel. It is paramount that the heat stratification stays intact in order for the Ecovat to function optimally.

1.1. Objectives

The goal of this assignment is to mathematically describe the possibly turbulent movements caused by heating the water inside the vessel and simulate these movements. Multiple scenarios will be simulated in order to research the consequences of the heating on the heat stratification in the vessel. These simulations will be conducted in IFISS, a Matlab package for solving flow problems.

The main research question thus becomes: does the heat stratification remain intact when adding heat and can this be simulated in IFISS?

This question will be answered using these subquestions:

- How can turbulence be described mathematically and what models can be used?
- What problems is IFISS suited for?
- What numerical techniques are used in IFISS?
- How can IFISS be adjusted to fit the necessary conditions?

1.2. Dimensions of the vessel

An Ecovat can have different sizes, although the heights are all 16 meters. The Ecovat under research is the one that is built in Uden. This vessel is of type small and has a diameter of 11

*Thanks to our supervisors Bernard Geurts and Gijs de Goeijen.

meters.

2. Buoyancy

2.1. Introduction

The water in the Ecovat will be *nonisothermal*, meaning that the temperature of the water will not be constant. When temperature increases, liquids generally get 'thinner' and therefore tend to flow more easily. This means that the viscosity of liquids generally decreases when temperature increases. Also, liquids usually expand when temperature rises, meaning a decrease in density of the liquid.
Since density decreases due to increasing temperature, heated water will flow to the top of the Ecovat. In some situations, not necessarily including Ecovat, temperature changes can have a significant influence on the flow field of the liquid. Temperature, in turn, is influenced by the flow field because of heat transport in the liquid.
This upward force caused by density differences is an example of buoyancy. Since heating and cooling of water plays a large role in the Ecovat, the effects of buoyancy cannot be overlooked. The bouyancy will be modeled into the Navier-Stokes equations using the Boussinesq approximation.

2.2. Boussinesq approximation

2.2.1 Navier-Stokes equations and continuity equation

The Navier-Stokes equations describe the motion of fluids. For the sake of simplicity, we will consider incompressible fluid flows. The equations for incompressible flows are given below.

$$\rho\left(\frac{\partial \mathbf{u}}{\partial t} + \mathbf{u}\cdot\nabla\mathbf{u}\right) = -\nabla p + \nabla\cdot\mu(\nabla\mathbf{u} + (\nabla\mathbf{u})^T) + \rho\mathbf{g} \tag{1}$$

Here $\mathbf{u}$ is the fluid velocity, ρ is the fluid density, p is the fluid pressure and $\mathbf{g}$ is the acceleration due to gravity. The fluid velocity $\mathbf{u}$ consists of a horizontal movement of the flow u and a vertical movement v, both depending on the spatial coordinates x and y and the time t.

$$\mathbf{u} = \mathbf{u}(x,y,t) = \begin{pmatrix} u(x,y,t) \\ v(x,y,t) \end{pmatrix}$$

The continuity equation is as follows:

$$\frac{1}{\rho}\frac{D\rho}{Dt} + \nabla\cdot\mathbf{u} = 0 \tag{2}$$

This is equation is solved together with the Navier-Stokes equations.

2.2.2 Results of Boussinesq approximation

The main results of Boussinesq approximation [12] are the following.

1. The variation of density is ignored in the continuity equation and in the equations for horizontal motion;
2. This variation is accounted for in vertical motion as an activator of buoyancy;
3. The influence of the variation in pressure on the bouyancy equations and in the temperature equation can be neglected.

These simplifications slightly reduce the nonlinear nature of the Navier-Stokes equation, as can be seen in the next section.

2.2.3 Derivation of simplified Navier-Stokes equations and continuity equation

The first term of the continuity equation contains the material derivative of the density. This derivative computes the time rate of change of the pressure moving with the flow field. This term can be expanded as shown below.

$$\frac{1}{\rho}\frac{\mathrm{D}\rho}{\mathrm{D}t} = \frac{1}{\rho}\left(\frac{\partial \rho}{\partial t} + u\frac{\partial \rho}{\partial x} + v\frac{\partial \rho}{\partial y}\right) = \frac{1}{\rho}\left(\frac{\partial \rho}{\partial t} + \mathbf{u}\cdot\nabla\rho\right) \tag{3}$$

The first result mentioned in the previous section states that the variation of density is ignored in the continuity equation. This reduces equation (3) to zero, leaving $\nabla \cdot \mathbf{u}$ to equal zero as well. This result is also known as the incompressibility constraint.
Ignoring the density and pressure variations in all terms except for the vertical motion allows us to replace ρ by a constant density ρ_0 and allows us to ignore ∇p. This yields the following equation.

$$\rho_0\left(\frac{\partial \mathbf{u}}{\partial t} + \mathbf{u}\cdot\nabla\mathbf{u}\right) = \nabla\cdot(\mu(\nabla\mathbf{u} + (\nabla\mathbf{u})^T) + \rho\mathbf{g}$$

Assuming a constant viscosity μ, the term $\nabla\cdot(\mu(\nabla\mathbf{u} + (\nabla\mathbf{u})^T)$ can be simplified to $\mu\nabla^2\mathbf{u}$.
Defining the density variation with respect to the constant density ρ_0 as $\Delta\rho = \rho - \rho_0$ allows for more simplification. The buoyancy term $\rho\mathbf{g}$ becomes $(\rho_0 + \Delta\rho)\mathbf{g}$. When the change in buoyancy due to density variation $\Delta\rho\mathbf{g} = (\rho - \rho_0)\mathbf{g}$ is assumed to vary linearly with the change in temperature, the change in buoyancy can be rewritten as $(\rho - \rho_0)\mathbf{g} = -\rho_0\beta(T - T_0)\mathbf{g}$. Here β is the coefficient of thermal expansion.
Substituting the above mentioned information into the Navier-Stokes equations yields our final simplified version.

$$\rho_0\left(\frac{\partial \mathbf{u}}{\partial t} + \mathbf{u}\cdot\nabla\mathbf{u}\right) = \mu\nabla^2\mathbf{u} + \rho_0(1 - \beta(T - T_0))\mathbf{g} \tag{4}$$

Along with the results acquired from continuity equation.

$$\frac{D\rho}{Dt} = 0, \qquad \nabla\cdot\mathbf{u} = 0 \tag{5}$$

Besides these equations governing the movement of the flow, the change in temperature due to diffusion and convection is described by

$$\frac{\partial T}{\partial t} + \mathbf{u}\cdot\nabla T = \alpha\nabla^2 T \tag{6}$$

2.2.4 Nondimensionalization

Using a nondimensional solution to solution to the problem, one can describe many dimensional forms of the problem. Also when dimensionless numbers become very small, it is clear which terms vanish and hence the original problem can be approximated by much simpler problems. For the nondimensionalization process, equation (5) is divided by ρ_0 to obtain

$$\frac{\partial \mathbf{u}}{\partial t} + \mathbf{u} \cdot \nabla \mathbf{u} = \frac{\mu}{\rho_0} \nabla^2 \mathbf{u} + (1 - \beta(T - T_0))\mathbf{g} \tag{7}$$

The descriptions in the following table and the global idea of the nondimensionalization process are taken from [1].

Scaling parameter	Description	Primary dimension
L	Characteristic length	L
U	Characteristic speed	Lt^{-1}
f	Characteristic frequency	t^{-1}
g	Gravitational acceleration	Lt^{-2}
`	Characteristic temperature	Θ

Using the scaling parameters, the nondimensionalized parameters are defined as follows.

$$t^* = \mathrm{f}t \qquad \mathbf{x}^* = \frac{\mathbf{x}}{\mathrm{L}} \qquad \mathbf{u}^* = \frac{\mathbf{u}}{\mathrm{U}}$$

$$\mathbf{g}^* = \frac{\mathbf{g}}{\mathrm{g}} \qquad \nabla^* = \mathrm{L}\nabla \qquad \Delta T^* = \frac{(T - T_0)}{\theta}$$

Substituting the nondimensionalized parameters into equation (7) yields

$$\mathrm{Uf}\frac{\partial \mathbf{u}^*}{\partial t^*} + \frac{\mathrm{U}^2}{\mathrm{L}}(\mathbf{u}^* \cdot \nabla^* \mathbf{u}^*) = \frac{\mu}{\rho_0}\frac{\mathrm{U}}{\mathrm{L}^2}\nabla^{*^2}\mathbf{u}^* + \mathrm{g}\mathbf{g}^* - \beta\theta \mathrm{g}\Delta T^* \mathbf{g}^* \tag{8}$$

Knowing that ρ_0 has dimension mL^{-3}, μ has dimension $mt^{-1}L^{-1}$ and β has dimension Θ^{-1}, it is easily seen that every term in equation (8) has dimension Lt^{-2}. In order to nondimensionalize the equation it is multiplied by $\frac{\mathrm{L}}{\mathrm{U}^2}$, which has dimension $L^{-1}t^2$. This results in the the following equation.

$$\frac{\mathrm{fL}}{\mathrm{U}}\frac{\partial \mathbf{u}^*}{\partial t^*} + \mathbf{u}^* \cdot \nabla^* \mathbf{u}^* = \frac{\nu}{\mathrm{UL}}\nabla^{*^2}\mathbf{u}^* + \frac{\mathrm{gL}}{\mathrm{U}^2}\mathbf{g}^* - \frac{\text{fi`gL}^3}{\nu\alpha}\Delta T^* \mathbf{g}^* \tag{9}$$

The last term on the right hand side of equation (9) is obtained by using $U = \frac{\nu}{L}$ [2], where ν denotes the kinematic viscosity $\frac{\mu}{\rho_0}$. Equation (9), in turn, can be rewritten using dimensionless numbers.

$$\frac{\partial \mathbf{u}^*}{\partial t^*} + \mathbf{u}^* \cdot \nabla^* \mathbf{u}^* = \left[\frac{1}{\mathrm{Re}}\right]\nabla^{*^2}\mathbf{u}^* + \left[\frac{1}{\mathrm{Fr}^2} - \mathrm{Ra}\right]\Delta T^* \mathbf{g}^* \tag{10}$$

Note that the coefficient of the first term on the left hand side of the equation becomes one by using the definition of the characteristic frequency as explained below. In this equation the dimensionless numbers, being the Reynolds, Froude, and Rayleigh numbers, are defined as

$$[\mathrm{Re}] = \frac{\mathrm{UL}}{\nu} \qquad [\mathrm{Fr}] = \frac{\mathrm{U}}{\sqrt{\mathrm{gL}}} \qquad [\mathrm{Ra}] = \frac{\beta \mathrm{gL}^3\theta}{\nu\alpha}$$

An indication of the order of magnitude of these dimensionless numbers is given by filling in the parameters as follows. The units used are SI units.

- A density ρ_0 of 997 kg/m^3 and a viscosity μ of 0.89×10^{-3}kg/ms, resulting in a kinematic viscosity ν of 8.93 $\times10^{-7}$m^2/s;
- A characteristic length L of 16 m, the height of the Ecovat, and a characteristic speed U between 10^{-2}m/s and 10^{-1}m/s. Using a characteristic speed of $\frac{\nu}{L}$ results in a value for U of the order of 10^{-8} m/s, which is not considered useful for this scenario;
- The characteristic frequency f will be defined as $\frac{U}{L}$;
- The gravitational acceleration g has a value of 9.81 m/s^2;
- The characteristic temperature is defined as the difference between the warmest and coolest layers of the vessel: $T_H - T_C = 80$C. The reference temperature T_0 is defined as the mean of the beforementioned layers: $\frac{T_H+T_C}{2} = 50$C.;
- The thermal expansion coefficient β has a value of 2.5×10^{-4} /K and the thermal diffusion coefficient α has a value of 0.143×10^{-6} m^2/s.

The values of the nondimensional numbers are thus:

- $[\mathrm{Re}] \approx 1.79 \times 10^5$ for $\mathrm{U} = 10^{-2}$ and $[\mathrm{Re}] \approx 1.79 \times 10^6$ for $\mathrm{U} = 10^{-1}$;
- $[\mathrm{Fr}] \approx 7.98 \times 10^4$ for $\mathrm{U} = 10^{-2}$ and $[\mathrm{Fr}] \approx 7.98 \times 10^3$ for $\mathrm{U} = 10^{-1}$;
- $[\mathrm{Ra}] \approx 6.23 \times 10^{15}$.

The ratio of the Grashof number to the square of the Reynolds number is used to predict whether forced or free (natural) convection effects may be neglected [9]. This ratio is calculated in the following way:

$$\frac{[\mathrm{Gr}]}{[\mathrm{Re}]^2} = \frac{[\mathrm{Ra}]/[\mathrm{Pr}]}{[\mathrm{Re}]^2} \tag{11}$$

Assuming a Prandtl number value of 7 [9], this ratio lies between 6.2 and 6.2×10^2. Thus the outcome of (11) is larger than 1 and could possibly be some orders of magnitude larger, meaning that free convection effects play a larger role than forced convection effects and that the latter might be neglected without large consequences.

The scaling parameters used to nondimensionalize the flow equations (7) are used as well to nondimensionalize the temperature diffusion-convection equation (6). Here it is used that $T = \theta\Delta T^* - T_0$. Equation (6) can thus be rewritten as stated below.

$$\mathrm{f}\theta\frac{\partial\Delta T^*}{\partial t^*} + \frac{\mathrm{U}\theta}{\mathrm{L}}\mathbf{u}^* \cdot \nabla^*\Delta T^* = \frac{\alpha\theta}{\mathrm{L}^2}{\nabla^*}^2\Delta T^* \tag{12}$$

Every term in (12) has dimension Θt^{-1}. Multiplying this equation by $\frac{\mathrm{L}}{\mathrm{U}\theta}$ yields a nondimensionalized equation, which is the following.

$$\frac{\partial\Delta T^*}{\partial t^*} + \mathbf{u}^* \cdot \nabla^*\Delta T^* = \left[\frac{1}{\mathrm{Pe}}\right]{\nabla^*}^2\Delta T^* \tag{13}$$

Here [Pe] denotes the Péclet number, defined as $\frac{\mathrm{UL}}{\alpha}$. The number has a value between 1.119×10^6 and 1.119×10^7, depending on the value of U.

2.2.5 Validity of the Boussinesq approximation

Gray and Georgini [8] look into Rayleigh-Bénard convection where θ is defined as the temperature difference along the vertical layer of the fluid. The range of validity of the approximate equations is stated below. Gray and Georgini conclude that the Boussinesq approximation can be valid for scenarios with a Rayleigh number up to 2.35×10^{19}. It is assumed here that $T_0 = 15$C, which is lower than in the Ecovat, and the pressure is 1 atm.

$$\theta \leq 1.25\text{C}$$
$$Ł \leq 2.4 \times 10^3\text{m}$$
$$\frac{L}{\theta} \leq 9.9 \times 10^2\text{m/C}$$

It is clear that only the first constraint is not satisfied. However, it is assumed that this will not pose a problem, as the Rayleigh number for the Ecovat scenario is very small compared to the maximum valid Rayleigh number.

3. Closure problems

3.1. Reynolds averaging

Reynolds averaging is a mathematical technique used to simplify the Navier-Stokes equations. This is done by decomposing variables into a mean and a fluctuating part. There are several forms of Reynolds averaging, from these forms time averaging is considered to be the most appropriate for engineering problems. Therefore this will be the only form considered in this article. The text in this subsection closely follows along the lines of Wilcox et al. [11].

Recall that a two-dimensional flow $\mathbf{u}$ dependent on the position (x, y) and the time t was given by

$$\mathbf{u} = \mathbf{u}(x, y, t) = \begin{pmatrix} u(x, y, t) \\ v(x, y, t) \end{pmatrix}$$

The velocities u and v can be expressed as the sum of an average part $U(x, y)$ and $V(x, y)$ and a fluctuating part $u'(x, y, t)$ and $v'(x, y, t)$. The time-averaged velocity is defined by

$$U(x, y) = \bar{u}(x, y, t) = \lim_{T\to\infty} \frac{1}{T} \int_t^{t+T} u(x, y, t)dt \tag{14}$$

Using this definition, some interesting properties can be deduced. Only the x-directed component of the flow is used to demonstrate these properties, but these also hold for the y-directed component.

$$\overline{U}(x, y) = \lim_{T\to\infty} \frac{1}{T} \int_t^{t+T} U(x, y)dt = U(x, y) \tag{15}$$
$$\overline{u'}(x, y, t) = \lim_{T\to\infty} \frac{1}{T} \int_t^{t+T} (u(x, y, t) - U(x, y))dt = U(x, y) - \overline{U}(x, y) = 0 \tag{16}$$

As it is impossible in practice to let T go towards infinity, it should be chosen such that it is very long compared to the maximum period of velocity fluctuations. This leads to the next property of time averaging of nonstationary turbulence.

$$\begin{aligned}\overline{\frac{\partial u}{\partial t}} &= \lim_{T\to\infty} \frac{1}{T}\int_t^{t+T} \frac{\partial}{\partial t}(U+u')dt \\ &= \frac{U(x,y,t+T)-U(x,y,t)}{T} + \frac{u'(x,y,t+T)-u'(x,y,t)}{T}\end{aligned} \tag{17}$$

The last term of equation (18) vanishes as T practically approaches infinity on the scale of the fluctuations. In the first term on the right hand side of equation (18), T is very small relative to the scale of the mean flow, i.e. T practically approaches zero. Thus,

$$\overline{\frac{\partial u}{\partial t}} = \frac{\partial U}{\partial t} \tag{18}$$

Given the time average of the product of two properties ϕ and ψ, the following can be derived.

$$\overline{\phi\psi} = \overline{(\Phi+\phi')(\Psi+\psi')} = \overline{\Phi\Psi + \Phi\psi' + \Psi\phi' + \phi'\psi'} = \Phi\Psi + \overline{\phi'\psi'} \tag{19}$$

The simplification is built on the fact that the product of the time average of a variable and the fluctuating part of a variable has a zero mean.

3.2. Reynolds-averaged Navier-Stokes equations

Recall from section 2.2.3 that the simplified equations for conservation of mass and momentum for incompressible flows are given by

$$\nabla\cdot\mathbf{u} = 0 \tag{20}$$

$$\rho_0\left(\frac{\partial\mathbf{u}}{\partial t} + \mathbf{u}\cdot\nabla\mathbf{u}\right) = \mu\nabla^2\mathbf{u} + \rho_0(1-\beta(T-T_0))\mathbf{g} \tag{21}$$

The convective term can be rewritten using equation (20) to simplify the averaging process:

$$\mathbf{u}\cdot\nabla\mathbf{u} = \nabla\cdot(\mathbf{u}\mathbf{u}^T) - (\nabla\cdot\mathbf{u})\mathbf{u} = \nabla\cdot(\mathbf{u}\mathbf{u}^T) \tag{22}$$

Combining this result with equation (21) yields the Navier-Stokes equation in conservation form.

$$\rho\left(\frac{\partial\mathbf{u}}{\partial t} + \nabla\cdot(\mathbf{u}\mathbf{u}^T)\right) = \mu\nabla^2\mathbf{u} + \rho_0(1-\beta(T-T_0))\mathbf{g} \tag{23}$$

Time averaging these equations leads to the Reynolds-averaged equations of motion.

$$\nabla\cdot\mathbf{U} = 0 \tag{24}$$

$$\rho\left(\frac{\partial\mathbf{U}}{\partial t} + \nabla\cdot(\mathbf{U}\mathbf{U}^T + \overline{\mathbf{u}'\mathbf{u}'^T}\right) = \mu\nabla^2\mathbf{U} + \rho_0(1-\beta(T-T_0))\mathbf{g} \tag{25}$$

The only difference between the instantaneous momentum equations (21) and the time-averaged equations (25), ignoring the fact that all variables have been replaced by their average parts, is the appearance of the term $\overline{\mathbf{u}'\mathbf{u}'^T}$. It is necessary to know how to compute this term in order to compute all averaged properties of the flow. The term $-\rho_0\overline{\mathbf{u}'\mathbf{u}'^T}$ is known as the Reynolds-stress tensor and is denoted by τ.

It is clear that τ is a symmetric matrix and therefore consists of three independent components. This means that the averaging process has produced three additional variables, and no additional equations.
Thus, in the case of a two-dimensional flow, there are three unknown mean-flow variables: the pressure and two flow velocities; there are three more Reynolds-stress components unknown. The system of equations (24) and (25) only yields three equations. This means the system is not yet closed. Closure can be achieved by designing additional equation by modeling unknown variables in closure models. One of these models will be discussed in the next section.

3.3. The mixing-length hypothesis

The mixing-length hypothesis was put forth by Prandtl in 1925. It is an algebraic model, which are considered to be the simplest turbulence models. The model will be explained through an intuitive physical analogy, and through mathematical formulation.

3.3.1 Intuitive explanation

A conceptual analagy for the mixing length is the mean free path. This means a particle will travel an average distance until it collides with other particles. For the mixing-length model, it means that a fluid parcel will on average travel a distance l_{mix} before blending in with neighbouring parcels. In other words, turbulent fluid motion is modeled such that fluid particles coalesce into 'lumps' that cling together and move as a whole.

3.3.2 Mathematical formulation

In analogy to the molecular transport of momentum, as stated by Wilcox et al. [11],

$$\tau = \mu \nabla^2 \mathbf{u} = \frac{1}{2} \rho_0 v_{mix} l_{mix} \nabla^2 \mathbf{u} \tag{26}$$

Prandtl defined the mixing velocity as the following. This definition was based on dimensional analysis. Here A is a constant.

$$v_{mix} = A \cdot l_{mix} |\nabla^2 \mathbf{u}| \tag{27}$$

These equations lead to

$$\tau = \mu_T \nabla^2 \mathbf{u} \tag{28}$$

where μ_T is the eddy viscosity, defined as

$$\mu_T = \rho_0 l_{mix}^2 |\nabla^2 \mathbf{u}| \tag{29}$$

Thus, the eddy viscosity is expressed in terms of the mixing length.

4. Model summary

In short, the governing set of equations consist of the Reynolds-averaged Navier-Stokes equation. The eddy viscosity is defined as postulated by Prandtl in 1925. These equations must be solved along with the incompressibility constraint and the temperature equation for diffusion and convection.

$$\rho_0\left(\frac{\partial \mathbf{U}}{\partial t}+\nabla\cdot\mathbf{U}\mathbf{U}^{\mathbf{T}}\right)=(\mu+\mu_T)\nabla^2\mathbf{U}+\rho_0(1-\beta(T-T_0))\mathbf{g} \tag{30}$$

$$\mu_T=\rho_0 l_{mix}^2|\nabla^2\mathbf{U}| \tag{31}$$

$$\nabla\cdot\mathbf{U}=0 \tag{32}$$

$$\frac{\partial T}{\partial t}+\mathbf{U}\cdot\nabla T=\alpha\nabla^2 T \tag{33}$$

5. The lid driven cavity

In this section, a simple test case is investigated to better understand how IFISS works. The case involves a lid driven cavity, which is a square domain with a moving top lid. The top lid moves to the right, resulting in a clockwise rotating flow in the cavity.
The batchfile that is used with the parameters for this test case is NS3_batch.m. To use this batchfile, one needs to type `batchmode('NS3')`. The program then automatically solves the test case. A description of how to set up such a problem manually is given in appendix A.

5.1. A short study on grid refinement

While finite element subdivisions (an overview is shown in paragraph 5.1.1) and grid parameters were varied, all the other parameters were kept constant according to table 1. It must be noted that the Newton iteration stops after two iterations for all simulations. This happens because the nonlinear tolerance is not exceeded anymore.

Table 1: Parameter choice

Problem type	Lid driven cavity
Cavity type	Leaky
Viscosity parameter	0.02
# Picard iterations	2
# Newton iterations	4
Nonlinear tolerance	1.d-8
Uniform/exponential streamlines	Uniform

5.1.1 Discretizations

Four different discretizations are available for the lid driven cavity. Two of them are inf-sup stable and two of them are automatically stabilized in IFISS.

Stabilized element pairs:

- **$\mathbf{Q}_1$-$\mathbf{Q}_1$**. Uses $\mathbf{Q}_1$ approximation for velocity and for pressure on the same gridpoints;
- **$\mathbf{Q}_1$-$\mathbf{P}_0$**. Uses $\mathbf{Q}_1$ approximation for velocity and a constant approximation ($\mathbf{P}_0$) for pressure.

Inf-sup stable element pairs:

- **Q_2-Q_1**. Uses $\mathbf{Q}_2$ approximation for velocity and continuous $\mathbf{Q}_1$ approximation for pressure;
- **Q_2-P_{-1}**. Uses $\mathbf{Q}_2$ approximation for velocity and discontinuous $\mathbf{P}_{-1}$ approximation for pressure. The $\mathbf{P}_{-1}$ element contains the pressure and its x and y derivatives.

$\mathbf{Q}_1$ (bilinear quadrilateral) and $\mathbf{Q}_2$ (biquadratic quadrilateral) are two standard finite element approximation methods [6].
The four discretizations are visualized on uniform grids with the same grid parameter in figure 1. The open dots represent the velocity and the asterisks represent the pressure.

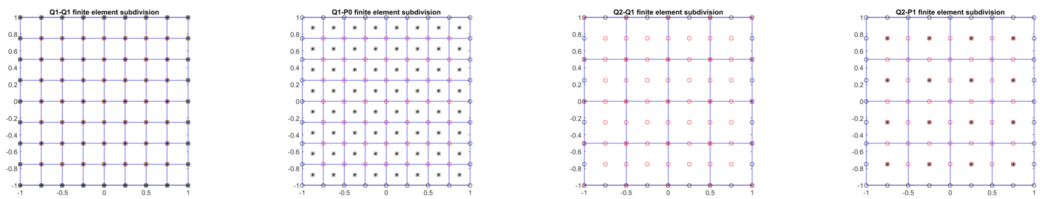

(a) (b) (c) (d)

Figure 1: Four different finite element subdivisions.

5.1.2 Solution plots

The standard graphic output that IFISS produces is a contour plot for the solutions of the velocity and pressure and a contour plot for the corresponding errors. When the grid parameter becomes larger, the solution plots seems to become more smooth (figure 2).

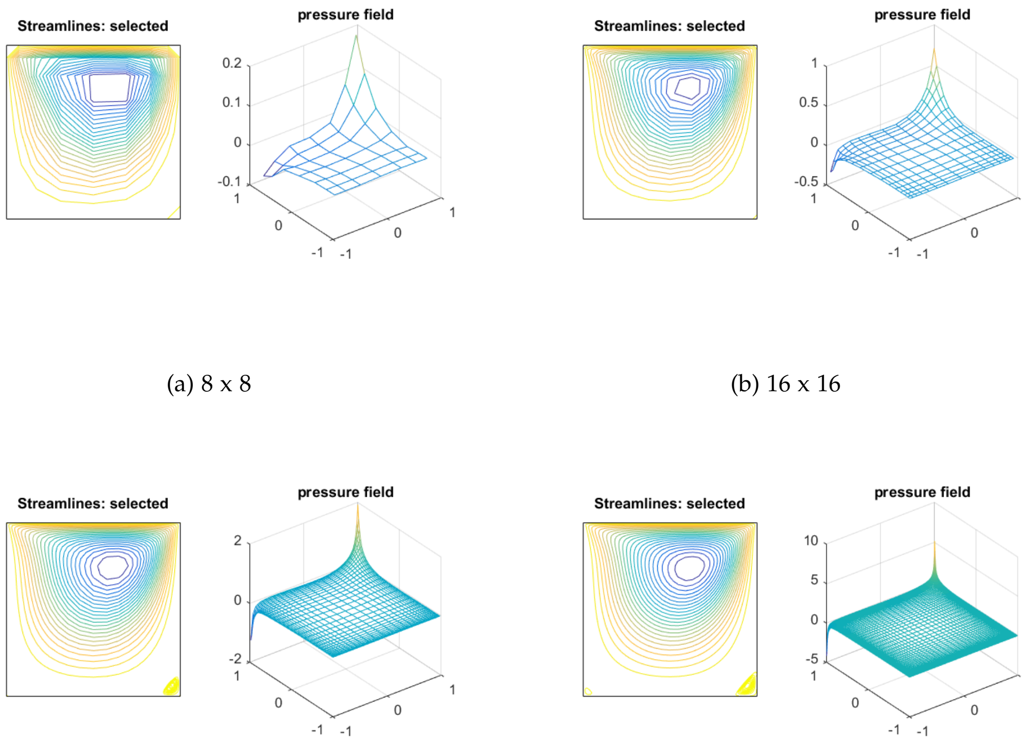

(a) 8 x 8

(b) 16 x 16

(c) 32 x 32

(d) 64 x 64

Figure 2: Solutions of the lid driven cavity on different Q_1-P_0 gridsizes

5.1.3 Solution vector

IFISS produces one solution vector, which contains the solutions for the x-velocity, y-velocity and pressure. The three parts of this vector can be seen as linearly indexed matrices for the three solution components. Depending on the discretization method the solution vector has different lengths. In table 2 the length of the three components of this vector is shown in terms of k, where $k = 2^n$, n being the grid parameter.

Discretization	x-velocity	y-velocity	Pressure
$\mathbf{Q}_1$-$\mathbf{Q}_1$	$(k+1)^2$	$(k+1)^2$	$(k+1)^2$
$\mathbf{Q}_1$-$\mathbf{P}_0$	$(k+1)^2$	$(k+1)^2$	k^2
$\mathbf{Q}_2$-$\mathbf{Q}_1$	$(k+1)^2$	$(k+1)^2$	$(k/2+1)^2$
$\mathbf{Q}_2$-$\mathbf{P}_{-1}$	$(k+1)^2$	$(k+1)^2$	$3 \cdot (k/2)^2$

Table 2: Lengths of the different components of the solution vector

5.1.4 Cross-sections

To check whether the solutions converge, vertical and horizontal cross-sections of the velocity solutions are plotted. These cross-sections are taken in the middle of the domain as indicated in figure 3.
The cross-sections seem to converge to a smooth curve as can be seen in figure 5. When looking at the boundaries of the cross sections and the behaviour inbetween, the velocities behave as expected. The flow vector field is plotted in figure 4 for more insight in the flow direction and velocity.

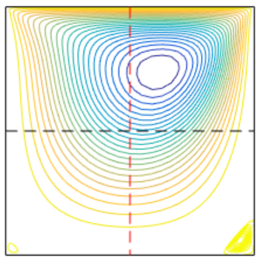

Figure 3: Cross-sections

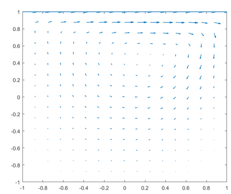

Figure 4: Stream direction of solution

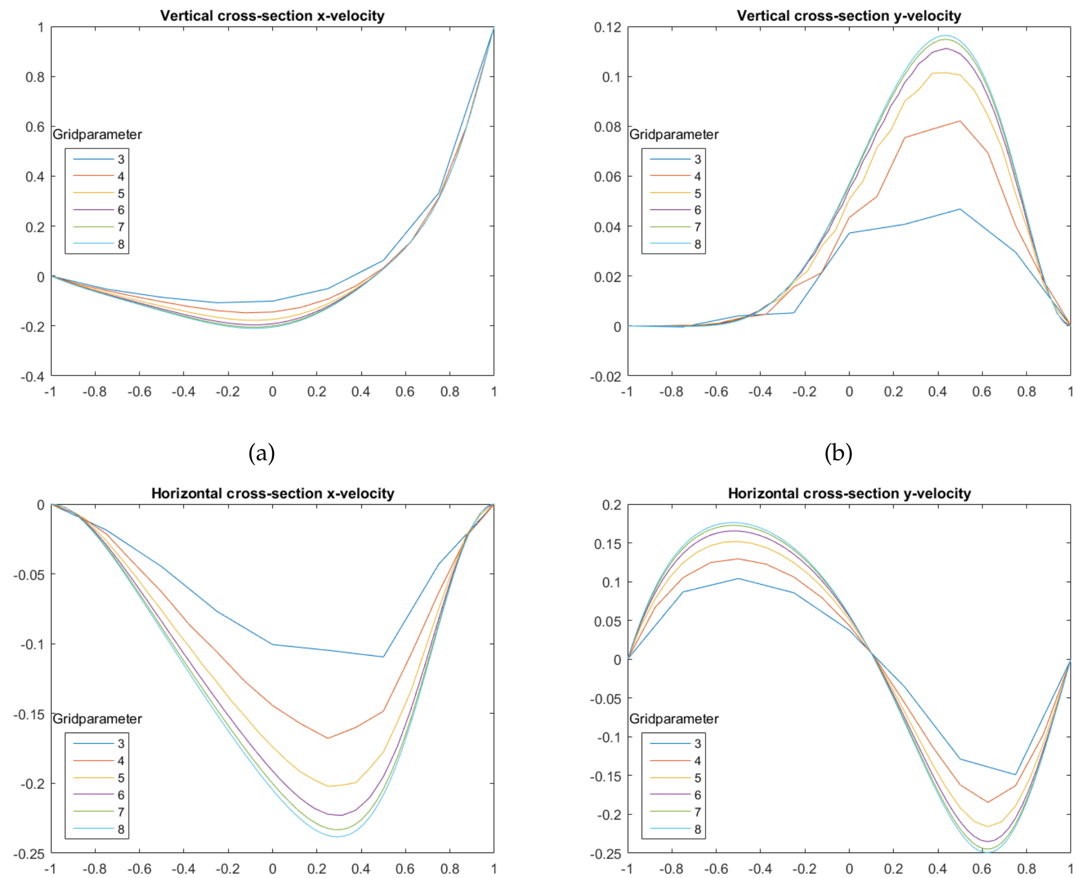

(a) (b)

(c) (d)

Figure 5: Vertical and horizontal cross-sections of the x-velocity and y-velocity with different grid parameters. The horizontal axes display the domain of the cross-sections, the vertical axes display the velocity on this domain.

5.1.5 Error convergence

Qualitatively, the solution seems to converge when refining the grid. To calculate the rate of convergence, a quantitative analysis of the errors is done.

Because of computational limitations, the highest grid parameter that could be used for simulations was 8. Therefore, the solution of this computation is assumed as the 'real' solution. The error compared to this solution is calculated for each of the lower grid parameters.

Stretched grids have a different stretch ratio per grid parameter, meaning that the solution points from different grid parameters do not have the same physical coördinates. The error analysis is therefore carried out on uniform grids. The L^2-norm is calculated for each of the physical coördinates, for each grid with grid parameters 3 to 7.
The errors for the four discretizations are plotted in figure 6. It can easily be seen that the errors become smaller as the grid parameters become bigger.

In figure 7 the Log2 of these errors is plotted. The rate of convergence seems to be of first order.

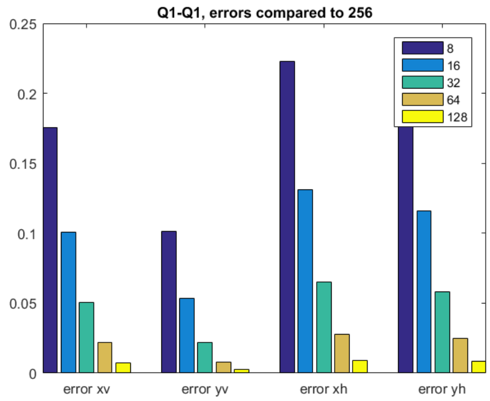

(a)

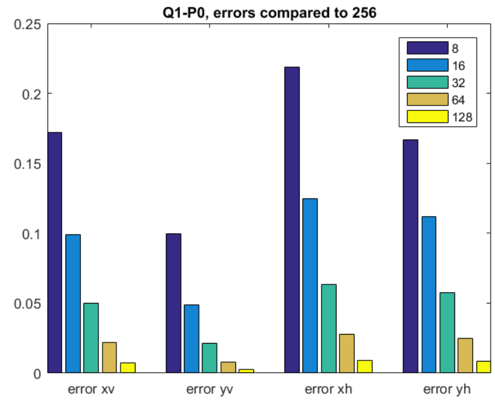

(b)

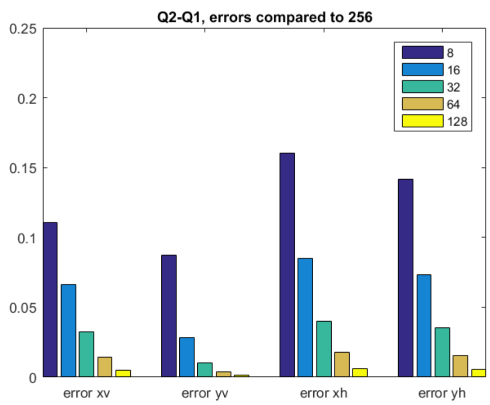

(c)

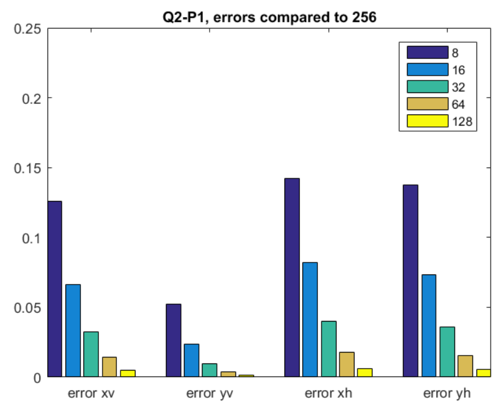

(d)

Figure 6: Vertical and horizontal cross-section errors of the x-velocity and y-velocity for different grid parameters, compared to the solution with grid parameter 8.

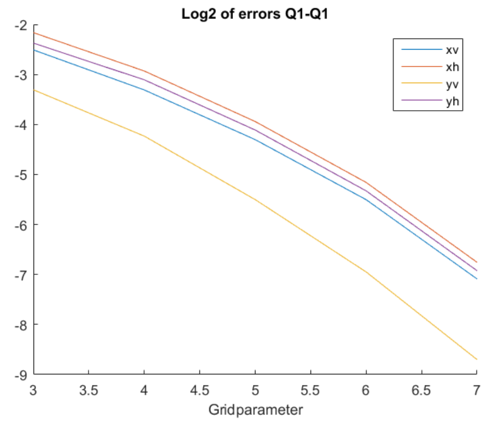

(a)

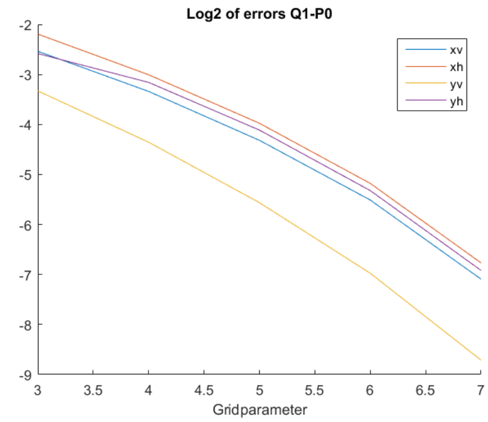

(b)

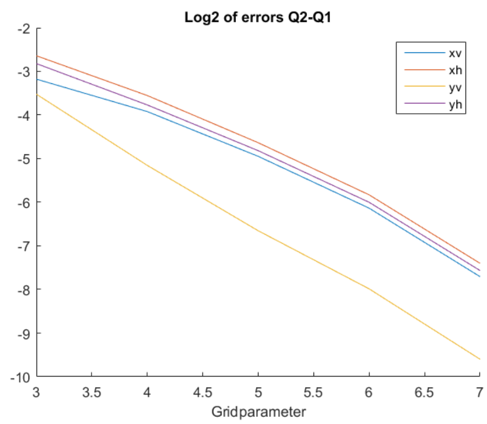

(c)

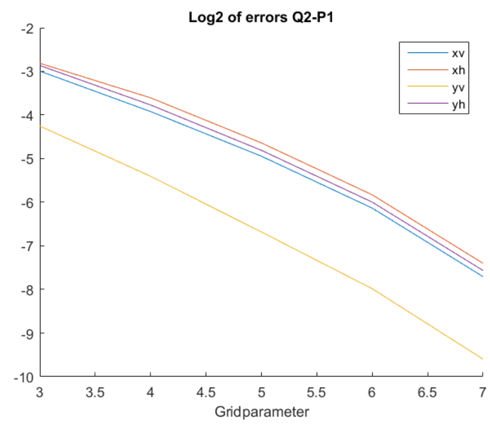

(d)

Figure 7: Log2 of the errors compared to grid parameter 8

6. Buoyancy-driven flow simulations in IFISS

6.1. Model

Besides the steady state solvers that are included in IFISS, the program offers an adaptive time-stepping algorithm for the simplest possible Boussinesq model of buoyancy driven flow [5]. The model is represented by the following system of PDEs:

$$\frac{\partial \mathbf{u}}{\partial t} + \mathbf{u} \cdot \nabla \mathbf{u} - \nu^* \nabla^2 \mathbf{u} + \nabla p = \mathbf{j} T \tag{34}$$

$$\nabla \cdot \mathbf{u} = \mathbf{0} \tag{35}$$

$$\frac{\partial T}{\partial t} + \mathbf{u} \cdot \nabla T - \nu \nabla^2 T = 0, \tag{36}$$

which must to be solved in $\mathcal{W} \equiv \Omega \times (0, \tau]$, where Ω is the flow domain and τ is the target time of the solution.

In these equations $\mathbf{u}$ denotes the fluid velocity, p the pressure and T the fluid temperature. $\mathbf{j}T$ is the term that represents the buoyancy force in the momentum equation and $\mathbf{j}$ is the unit vector in the y-direction.

The two different viscosity parameters ν^* and ν are defined as follows:

$$\nu^* = \sqrt{\frac{\mathrm{Pr}}{\mathrm{Ra}}}, \quad \nu = \frac{1}{\sqrt{\mathrm{Pr} \cdot \mathrm{Ra}}}, \tag{37}$$

Where Pr denotes the Prandtl number and Ra denotes the Rayleigh number. These viscosity parameters follow from the nondimensionalization process that has been followed [3]. The Prandtl number is a property of the fluid. A typical value for water is 7.1 [5]. The flow domain is taken $\Omega = [0, 11] \times [0, 16]$, according to the dimensions of the Ecovat vessel.

6.2. Boundary conditions

The boundary Γ consists of two non-overlapping pieces that cover the whole boundary: $\Gamma = \Gamma_D \cup \Gamma_N$, where Γ_D denotes the part of the boundary where Dirichlet conditions hold and Γ_N denotes the part of the boundary where Neumann conditions hold.

The problem type is that of an enclosed cavity flow. Therefore at every timestep the velocity on the boundary is 0, so

$$\mathbf{u} = \mathbf{0} \quad \text{on} \quad \Gamma \times (0, \o]. \tag{38}$$

At the heated or cooled parts of the boundary the Dirichlet boundary conditions hold:

$$T = T_g \quad \text{on} \quad \Gamma_D \times (0, \o], \tag{39}$$

where T_g is the designated temperature.

At the parts of the boundary where no heat is added or withdrawn the Neumann boundary conditions hold:

$$\nu \nabla T \cdot \mathbf{n} = 0 \quad \text{on} \quad \Gamma_N \times (0, \o], \tag{40}$$

where $\mathbf{n}$ is the normal vector pointing outwards to the boundary Γ_N. This condition models a perfectly insulated wall on these parts of the boundary.

6.3. Boussinesq flow in IFISS

`unsteady_bouss_testproblem.m` sets up a problem for buoyancy driven flow. `unpack_boussdata.m` sets up the data for Boussinesq flow problem. This also sets up the grid. `stabtrBouss.m` contains the robust version of the Boussinesq integrator using TR.

Unless otherwise stated, all simulations are carried out with the parameters in table 3.

Table 3: Relevant parameters for simulations

Domain height	16
Domain width	11
Grid type	Uniform
# elements in x direction	40
Multiplication factor in y direction	16/11
Node enumerate direction	y
Type of BC for the temperature on horizontal walls	Adiabatic (Neumann)
Rayleigh number	3.4e5
Prandtl number	7.1
Accuracy tolerance	3e-5
# nonlinear Picard iteration steps	0
Averaging frequency	10

6.3.1 Dirichlet and Neumann boundary conditions on vertical walls

The standard laterally heated cavity implemented in IFISS has the choice of Dirichlet or Neumann boundary conditions for the horizontal walls. The vertical walls however are assumed to have Dirichlet boundary conditions. Because only some parts of the vertical walls are heated or cooled, it is necassary to put Neumann boundary conditions on the isolated parts of the vertical walls.

This is done by removing the nodes in question from the vector ***bnd_dn2***, which contains the temperature boundary nodes that have assigned values. This is done in the `unpack_boussdata.m` file after the unpacking of this vector.

It is important to realise that the vector ***bc*** with boundary values that is copied to the `specific_bc.m` file now contains only the values that are assigned to the remaining temperature boundary nodes.

6.3.2 Switching from Neumann to Dirichlet boundary conditions at a given time

It is desirable to change the boundary conditions at a given time when simulating heating for a given amount of time. The easiest way to do this is to start with the desired Dirichlet boundary conditions which describe where the heat is added. At the given time where Dirichlet boundary conditions change into Neumann boundary conditions, the same node removal procedure is followed as described in section 6.3.1.

6.4. Grid refinement study

It is expected that a fine grid results in a more accurate simulation, as was shown with the lid driven cavity. A simple grid refinement study has been performed and will be explained here. Two cases are studied. The first case has a Rayleigh number of 3.4×10^2, which is expected to result in laminar flow only. The Rayleigh number for the second case is 3.4×10^5, which is expected to cause small eddies but no major turbulent flow. The specifics for both cases are given below.

The temperature and the velocities in x-direction and y-direction are compared in the center of the vessel, in a point in the left side of the lower layer, and in a point on the right side of the upper

Case	**1**	**2**
Vessel size	11×16	11×16
Initial temperature	Three-layered -0.5, 0, 0.5	Three-layered -0.5, 0, 0.5
Boundary temperature	Dirichlet, value 0	Dirichlet, value 0
Prandtl number	7.1	7.1
Rayleigh number	3.4×10^2	3.4×10^5
Target time	600	600

layer. These points are named point 1, point 2 and point 3 respectively from now on.
The errors are calculated by comparing the data every two simulated time units, and taking the square root of the sum of the squared differences between this data and the reference data.

First case

The data from the simulation using the 40×80 grid is used as reference data. This was the finest possible grid which data could be retrieved from.

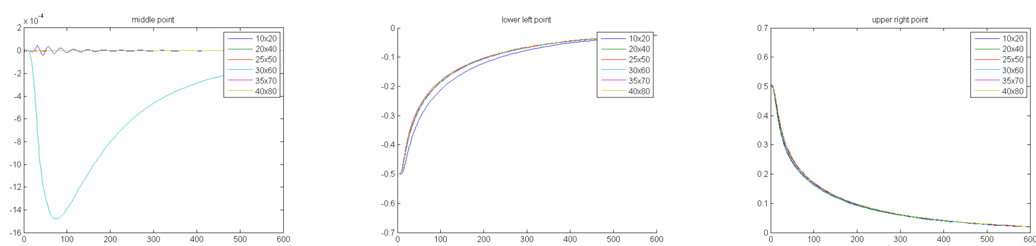

Figure 8: Temperature developments for points 1, 2 and 3

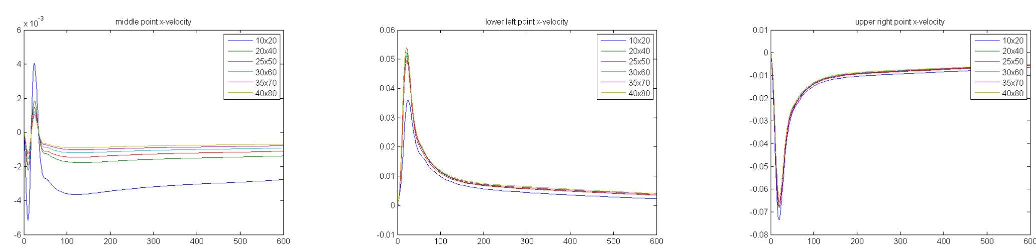

Figure 9: Velocity in x-direction for points 1, 2 and 3

It can be seen that the temperature and the velocity generally show the same behavior. Grid refinement does not result in a convergence to a certain solution, as is shown in figure 11.

Second case

The data from the simulation using the 40×80 grid is used as reference data. All simulations using grids coarser than the 25×50 grid did not reach the target time due to a rapid decrease in

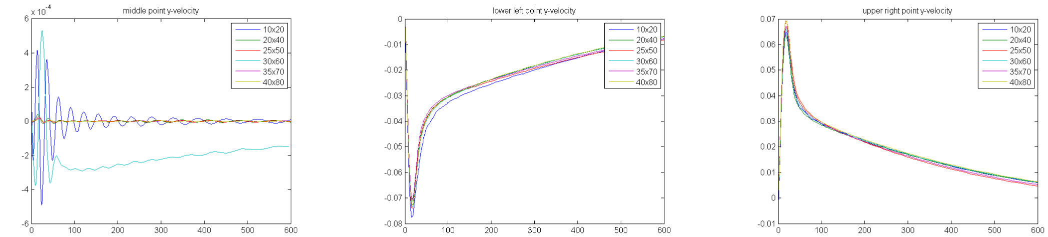

Figure 10: Velocity in y-direction for points 1, 2 and 3

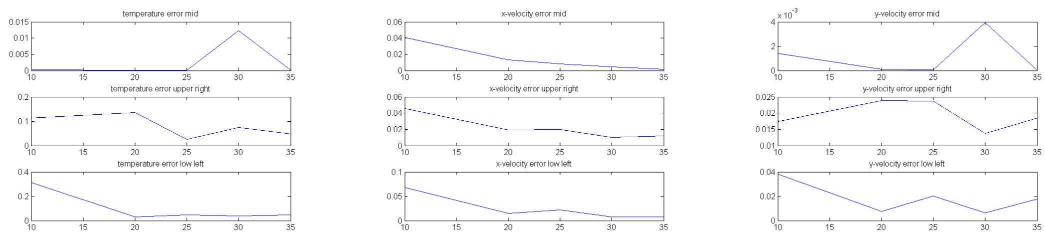

Figure 11: Errors in temperature, velocity in x-direction and velocity in y-direction

timestep size. This is most likely caused by the solution becoming unstable due to inaccuracies of the coarse grids. This data will therefore not be used.

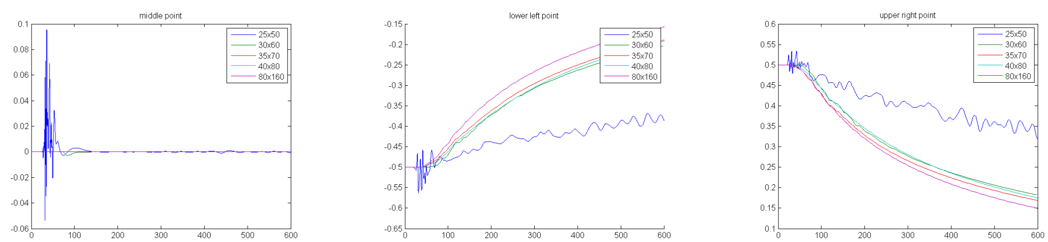

Figure 12: Temperature developments for points 1, 2 and 3

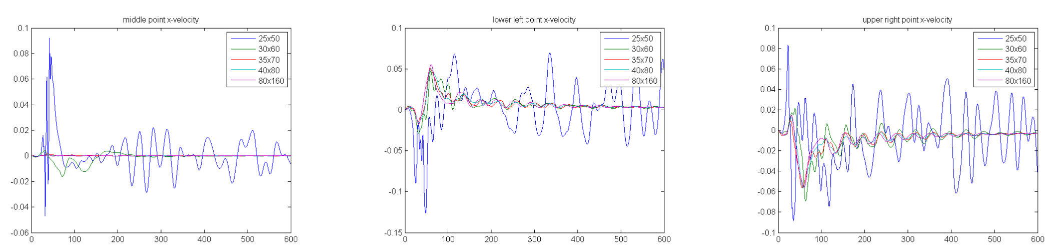

Figure 13: Velocity in x-direction for points 1, 2 and 3

The temperature shows the same behavior on all grids except for the 25×50 grid, which behaves in a more turbulent way. The same can be seen for the velocities in x-direction and y-direction. A converging trend shows, with the 35×70 and 40×80 showing very similar behavior, yet the

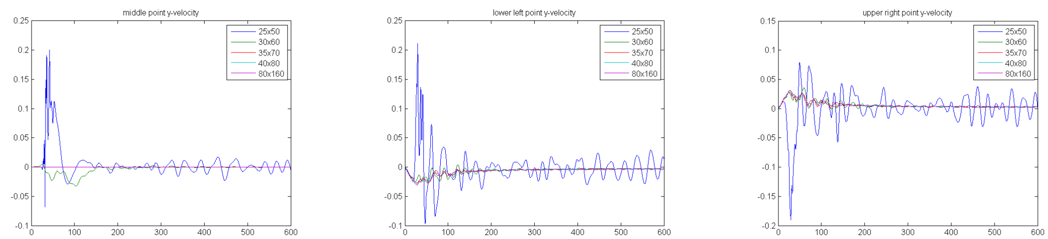

Figure 14: Velocity in y-direction for points 1, 2 and 3

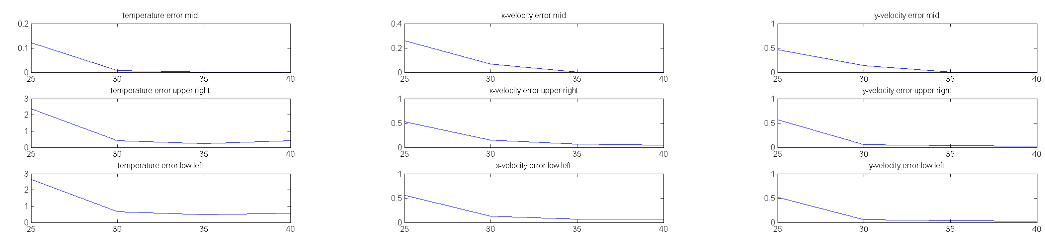

Figure 15: Errors in temperature, velocity in x-direction and velocity in y-direction

difference in temperature in points 2 and 3 is quite significant compared to the results from the 80×160 grid.

7. Ecovat simulations

This section describes the simulations performed in IFISS in order to best approximate the scenario of the Ecovat. The simulation settings can be found in table 3 in section 6.3.
It is possible to change many parameters when setting up a simulation. The most important parameters are the number of layers in the vessel, where to add or extract heat, and the duration of adding or withdrawing heat. For simplicity and to restrict the number of scenarios, a three-layered initial condition is chosen. For the other parameters a mixed choice is made to give some insight in the behavior of the temperature in the vessel that could be relevant for the problem in this study. Besides that, it is desirable to explain the solutions from a physical point of view.

The temperatures mentioned in the simulations are the nondimensionalized temperatures. The time showed here is dimensionless as well.
The snapshots give a qualitative overview of the movement of the temperature contour lines. Unless stated otherwise the snapshots are taken at nondimensionalized times $t = 0$, $t = 100$ and $t = 750$. Also a short description will be given for each situation.

1 **All the layers have the same temperature.**
In this example the water in the vessel has the same temperature everywhere. Neumann boundary conditions hold on all the boundaries, thus no energy is lost. As there are initially no temperature differences, the temperature stays constant and no movement of the water occurs. This results in the simulation of this scenario being finished very quickly (4 timesteps) and the solution is as predicted: the initial temperature remains stationary everywhere in the vessel.

2 **There is a linear temperature gradient, increasing from the bottom to the top of the vessel and no heat is added nor withdrawn.**

Very little movement can be observed. Comparing the first and the last figure shows that some diffusion has taken place.

The following examples make use of a cavity that is divided into three 'layers' and no heat is added nor withdrawn.

3 **The upper layer is hotter than the lower layers.**

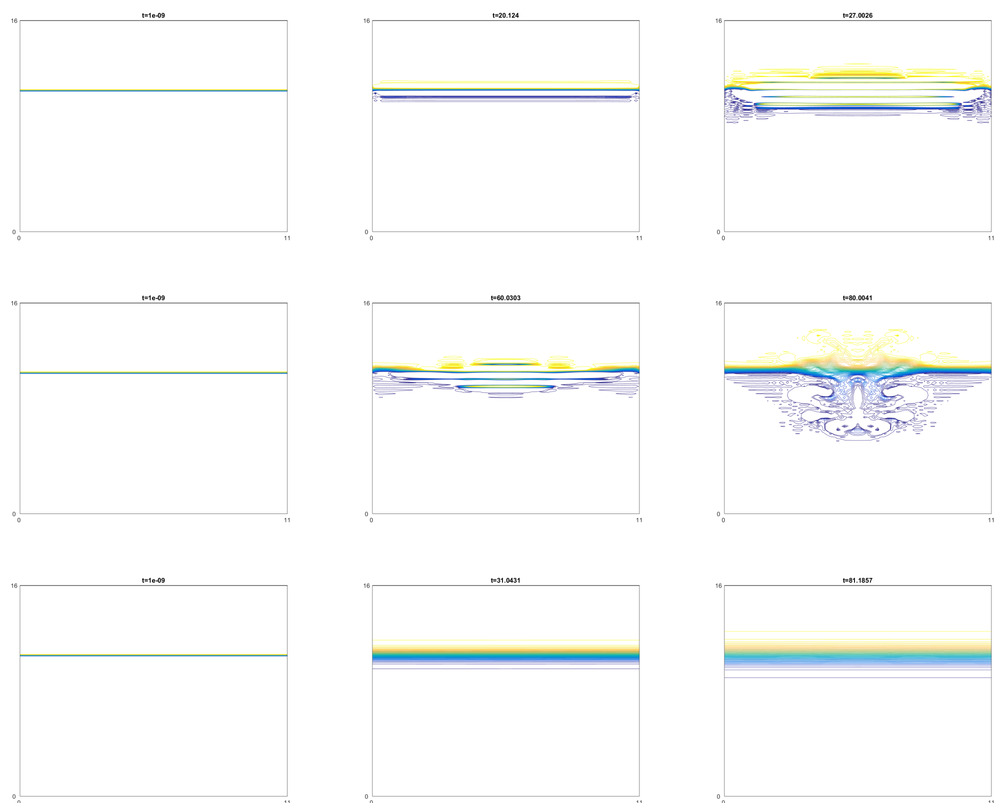

It is expected that the initial stratification in the vessel stays intact during this simulation. However, some irregularities show at the lower boundary of the upper layer. These irregularities are most likely caused by numerical inaccuracies. This effect disappears and thermal diffusion increases when the Rayleigh number decreases. This can be seen in the figures above, where the Rayleigh numbers are 3.4×10^5, 2.4×10^5 and 3.4×10^4 for the upper, middle, and lower rows of figures respectively. The irregularities also disappear when the temperature difference between the upper layer and the other layers is decreased.

4 **The upper layer is hotter than the middle layer, which in turn is hotter than the lower layer.**

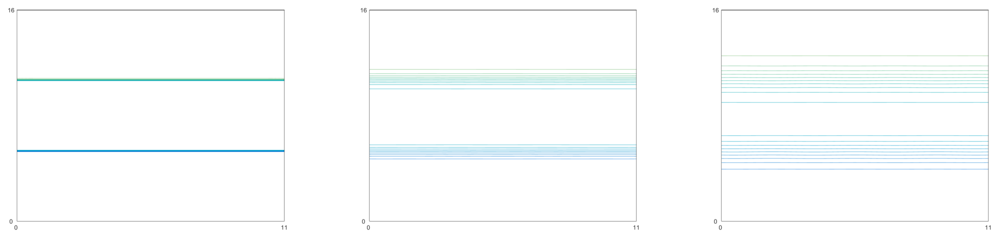

This example shows stable behavior, in contrast to 7. It must be noted here that the nondimensional temperatures of the layers are 0.1, 0.2 and 0.3 from the bottom to the top. Thermal diffusivity can easily be seen.

The following examples have the same initial conditions as example 7, but the heating process is different.

5 **Heat is added in the upper layer.**

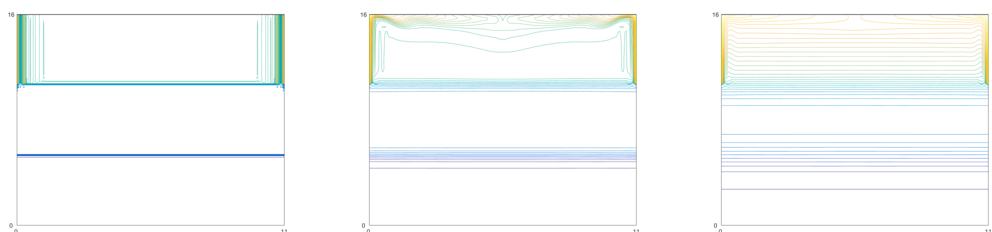

The heating causes the temperature of the upper layer to rise. Some thermal diffusion takes place, but the stratification remains intact and no turbulent movements are observed.

6 **Heat is added in the middle layer, but the heat element does not become hotter than the upper layer.**

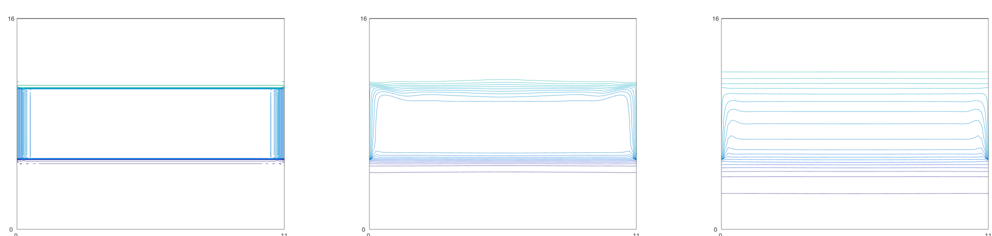

The heat can be seen to move up along the walls of the vessel until it reaches the boundary between the two upper layers. It then moves horizontally along the boundary and causes the temperature of the middle layer to increase. The top of the middle layer increases earlier than the bottom. The upper and lower layers of the vessel remain intact.

7 **Heat is added in the middle layer, and the heat element becomes hotter than the upper layer.**

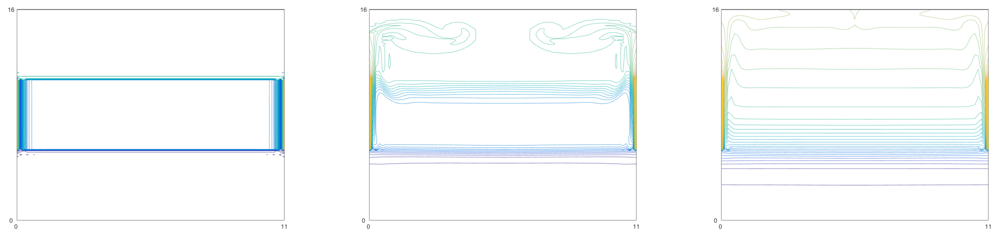

The heat travels up along the walls to the top of the vessel. Large eddies appear when the upper two layers are intact. The boundary between these layers disappears afterwards and the temperature gradually increases upwards from the lower boundary of the middle layers.

8 **Heat is added in the bottom layer, and the heat element becomes hotter than the middle layer but not as hot as the upper layer.**

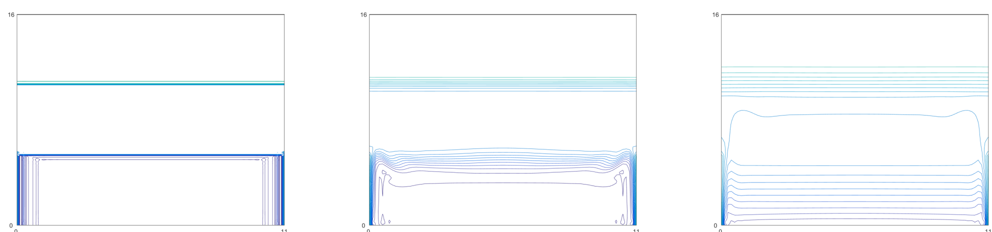

The behavior observed in this example is very similar to that of the previous example. The heating does not break the boundary between the upper two layers, instead the upper layer stays intact.

9 **Heat is added in the bottom layer, and the heat element becomes hotter than the upper layer.**

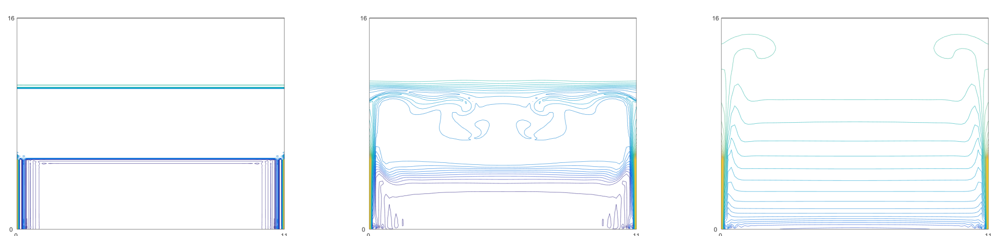

The boundary between the lower and the middle layers quickly vanishes. The lower boundary of the upper layer stays intact for some time, but is expected to vanish as time increases.

The following examples have the same initial conditions and heating temperature as example 7, but the heating duration is varied. Heat is added from $t = 0$ to the times given below.

10 **Heat is added in the middle layer until time** $t = 80$

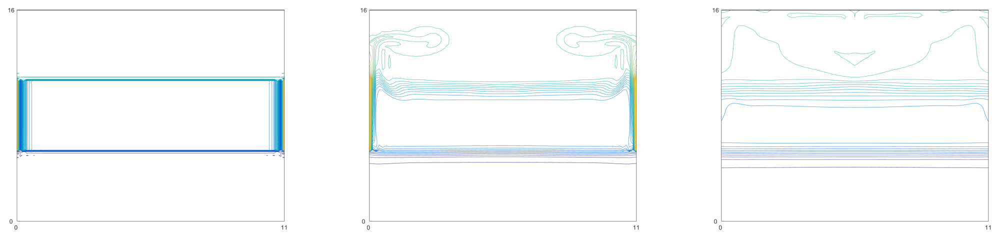

11 **Heat is added in the middle layer until time** $t = 160$

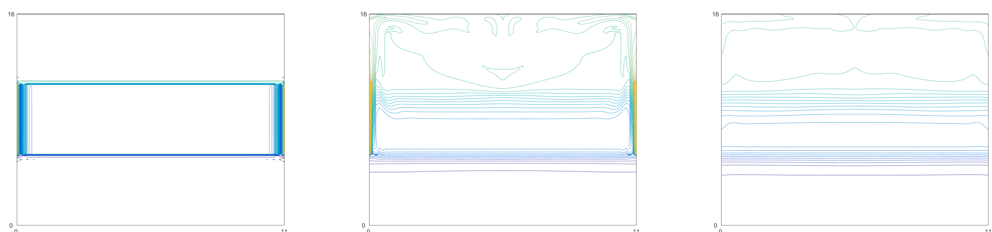

12 **Heat is added in the middle layer until time** $t = 320$

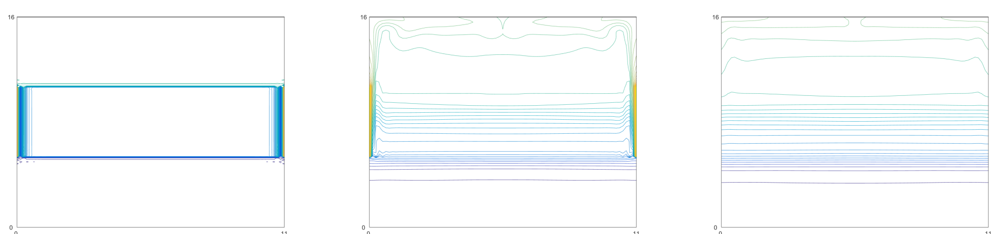

13 **Heat is added in the middle layer until time** $t = 640$

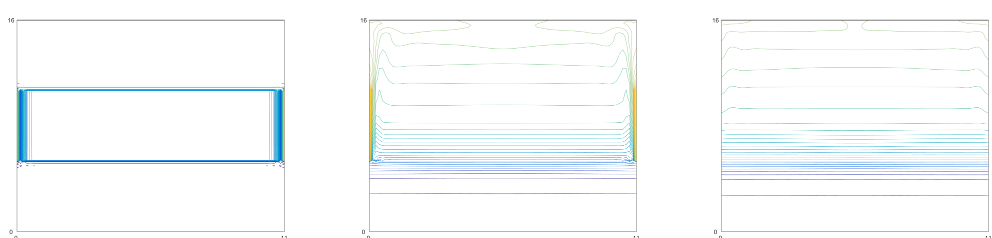

Examples 10, 11, 12 and 13 all show the same behavior. Some turbulent movements can be observed in the upper layer, despite the heating taking place at the middle layer. Heating during 80 time units causes the stratification to remain intact except for some diffusion at the boundaries. Heating for longer periods of time results in the boundary between the two upper layers to become increasingly harder to detect.

7.1. Simulation overview

Overall the solutions of the example scenarios do not show unexpected physical behavior. Hot water moves towards the top of the vessel and as a result cold water moves down.
It seems that the development of large eddies is not happening. The heated water travels mainly along the walls of the vessel and then it spreads along the top of the vessel or along a hotter temperature layer and moves downwards along the central vertical axis of the vessel. In the stable situations, such as the temperature gradient or the stratification with the hottest layer on top, the diffusion of the heat is well observed. We must mention here that these simulations are carried out at relatively low Rayleigh numbers. At higher Rayleigh numbers the calculations become more expensive as small eddies appear faster. This effect can be seen in example 3 of the simulations.
It is interesting to see that when adding heat in a layer in a smart manner, the heating does not affect the stratification. Instead the effect of diffusion plays a stronger role due to the larger temperature differences that appear.

8. Conclusion

In this report we have combined existing models into a turbulence model that describes buoyancy driven flows. This model is based on the Boussinesq approximation and Prandtl's mixing-length model. Even though this model was designed on paper, too little time was available to try to implement this in IFISS.
The built-in Boussinesq model for buoyancy-driven flow of IFISS formed the basis to simulating the Ecovat in two dimensions. IFISS has been adjusted to approximate the Ecovat as best as possible. Multiple scenarios have been examined and qualitative analysis has been performed.
The outcomes of the simulations show physically feasible processes taking place in the Ecovat. Heating in a smart manner allows the addition of energy to the vessel without breaking the stratification.

9. Discussion

The following points require some attention.

- The theoretical model which was developed using the Boussinesq approximation and Prandtl's mixing-length model is obviously not perfect. The Boussinesq approximation is an abstraction of reality, since a lot of terms are ignored. However, it forms the basis of most solutions to natural convection problems. Prandtl's mixing-length model is a turbulence model which is known to be incomplete, but was chosen because it was among the easiest models to understand and to implement.
- IFISS uses other equations than the one posed in this report to solve flow problems. Implementation of the developed model was not possible due to time constraints. The analysis performed on the model might therefore not be fully applicable to the model on which IFISS is based.
- The model is designed to describe a two-dimensional flow and should be easily extendable to three dimensions. IFISS is only suited for two-dimensional flows, which differ a lot from three-dimensional flows. The exact outcomes of the simulation will obviously not

replicate the real scenario, but the trends observed should be very similar. An appropriate way to solve this is by assuming the vessel is fully axi-symmetrical, which reduces the three-dimensional problem to a two-dimensional problem.

- All variables in IFISS were nondimensionalized. This made it hard to find out what real values the variables represented and which values had to be used for the nondimensional numbers. This was solved by only analysing qualitative behavior of the water. La Quéré and Behnia [10] have shown that smaller values of the Rayleigh number are often used when computing solutions for large values of the parameter and that the solutions are usually similar. Therefore it is assumed that too significant a difference in the Rayleigh number should not pose a problem for qualitative analysis.

9.1. Recommendations for further research

If further research on the water movement inside the Ecovat is conducted, we recommend the using powerful numerical solvers to simulate the Ecovat in three dimensions. Three-dimensional simulations will approximate the real situation even further, especially since the axi-symmetrical constraint is lifted.
Three-dimensional simulation can be achieved by either using existing software or creating code from scratch. The former might take time to fully understand and adjust according to the problem. The latter requires in-depth knowledge of computational fluid dynamics and takes time to develop and validate.

If research for the Ecovat using IFISS is continued, we recommend to try implement turbulence models such as Prandtl's mixing-length model and compare the results with our results.

Once the Ecovat is operational and test data is available, it is strongly recommended to compare simulation outcomes with the test data in order to validate the models used.

References

[1] Y. A. Cengel, J. M. Cimbala, et al. *Fundamental and applications*. McGraw Hill, New York, 2006.

[2] I. Cherkashin. Boussinesq approximation and nondimensionalization for mantle convection, March 2016.

[3] M. A. Christon, P. M. Gresho, and S. B. Sutton. Computational predictability of time-dependent natural convection flows in enclosures (including a benchmark solution). *International Journal for Numerical Methods in Fluids*, 40(8):953–980, 2002.

[4] H. C. E. D. J. Silvester and A. Ramage. Incompressible flow iterative solution software (ifiss) installation and software guide, version 3.5. `http://www.maths.manchester.ac.uk/~djs/ifiss/ifiss_guide_3.5.pdf`, 2016.

[5] H. Elman, M. Mihajlović, and D. Silvester. Fast iterative solvers for buoyancy driven flow problems. *Journal of Computational Physics*, 230(10):3900–3914, 2011.

[6] H. Elman, A. Ramage, and D. Silvester. Algorithm 866: IFISS, a Matlab toolbox for modelling incompressible flow. *ACM Trans. Math. Softw.*, 33:2–14, 2007.

[7] H. C. Elman, D. J. Silvester, and A. J. Wathen. *Finite elements and fast iterative solvers: with applications in incompressible fluid dynamics*. Oxford University Press (UK), 2014.

[8] D. D. Gray and A. Giorgini. The validity of the boussinesq approximation for liquids and gases. *International Journal of Heat and Mass Transfer*, 19(5):545 – 551, 1976.

[9] F. P. Incropera. *Fundamentals of Heat and Mass Transfer*. John Wiley & Sons, 2006.

[10] P. Le QuéRé and M. Behnia. From onset of unsteadiness to chaos in a differentially heated square cavity. *Journal of Fluid Mechanics*, 359:81âĂŞ107, 1998.

[11] D. C. Wilcox et al. *Turbulence modeling for CFD*, volume 2. DCW industries La Canada, CA, 1998.

[12] R. K. Zeytounian. Joseph boussinesq and his approximation: a contemporary view. *Comptes Rendus Mecanique*, 331(8):575–586, 2003.

A. Manually create problem scenarios in IFISS

This file executes the solver with the parameters given in the batchfile. When this file is run on its own, the program asks for the input parameters rather than execute it directly from the batchfile. The script can be found in the directory: ...ifiss3.5\navier_flow\test_problems\navier_testproblem.m

When running navier_testproblem.m, the following parameters must be entered:

- First make a choice for a specific example:
  1. Channel domain
  2. Flow over a backward facing step
  3. Lid driven cavity (default)
  4. Flow over a plate
  5. Flow over an obstacle
  6. Flow in a symetric step channel
- Next choose a cavity type:
  1. Leaky
  2. Tight
  3. Regularised (default)

Now the program knows the problem which it must handle and accordingly copies the corresponding files with specific boundary conditions to the files stream_bc.m and specific_flow.m.

- Choose the grid parameter: this must be an integer $n \geq 2$. The created grid is a 2^nx2^n grid, where the default grid size is 16x16.
- Choose the grid type:
  1. Uniform (default)
  2. Stretched
- Choose the discretization method:
  1. Q1-Q1
  2. Q1-P0 (default)
  3. Q2-Q1
  4. Q2-P1

The program now builds the desired grid structure

- The entry is the viscosity parameter, which can be any positive number with a default value of 1/100.
- The type of linearization is asked:
  1. Picard
  2. Newton

3. Hybrid (default)

- The next parameters are the number of Picard iterations, with a default of 3, the number of Newton iterations, with a default of 5, and the nonlinear tolerance, with a default value of $1.1 \times \text{eps}$.
- The last input is the type of streamlines:
  1. Uniform (default)
  2. Nonuniform

The program now has all necessary information to solve the given problem.